POLITECNICO DI TORINO
Repository ISTITUZIONALE

Channeling anabolic side-products towards the production of non-essential metabolites: stable malate production in Synechocystis sp. PCC6803

Original
Channeling anabolic side-products towards the production of non-essential metabolites: stable malate production in Synechocystis sp. PCC6803 / Battaglino, Beatrice; Du, Wei; Pagliano, Cristina; Jongbloets, Joeri A; Re, Angela; Saracco, Guido; Branco dos Santos, Filipe. - In: ACS SYNTHETIC BIOLOGY. - ISSN 2161-5063. - STAMPA. - 10:12(2021), pp. 3518-3526. [10.1021/acssynbio.1c00440]

Availability:
This version is available at: 11583/2947693 since: 2021-12-23T12:42:50Z

Publisher:
ACS Publications

Published
DOI:10.1021/acssynbio.1c00440

Terms of use:

This article is made available under terms and conditions as specified in the corresponding bibliographic description in the repository

Publisher copyright
ACS postprint/Author's Accepted Manuscript

This document is the Accepted Manuscript version of a Published Work that appeared in final form in ACS SYNTHETIC BIOLOGY, copyright © American Chemical Society after peer review and technical editing by the publisher. To access the final edited and published work see http://dx.doi.org/10.1021/acssynbio.1c00440.

(Article begins on next page)

06 May 2026

ACS SyntheticBiology

pubs.acs.org/synthbio

Research Article

Channeling Anabolic Side Products toward the Production of Nonessential Metabolites: Stable Malate Production in *Synechocystis* sp. PCC6803

Beatrice Battaglino,[‖] Wei Du,[‖] Cristina Pagliano, Joeri A. Jongbloets, Angela Re, Guido Saracco, and Filipe Branco dos Santos*

Cite This: *ACS Synth. Biol.* 2021, 10, 3518–3526

Read Online

ACCESS | Metrics & More | Article Recommendations | Supporting Information

ABSTRACT: Powered by (sun)light to oxidize water, cyanobacteria can directly convert atmospheric CO_2 into valuable carbon-based compounds and meanwhile release O_2 to the atmosphere. As such, cyanobacteria are promising candidates to be developed as microbial cell factories for the production of chemicals. Nevertheless, similar to other microbial cell factories, engineered cyanobacteria may suffer from production instability. The alignment of product formation with microbial fitness is a valid strategy to tackle this issue. We have described previously the "FRUITS" algorithm for the identification of metabolites suitable to be coupled to growth (i.e., side products in anabolic reactions) in the model cyanobacterium *Synechocystis*. sp PCC6803. However, the list of candidate metabolites identified using this algorithm can be somewhat limiting, due to the inherent structure of metabolic networks. Here, we aim at broadening the spectrum of candidate compounds beyond the ones predicted by FRUITS, through the conversion of a growth-coupled metabolite to downstream metabolites via thermodynamically favored conversions. We showcase the feasibility of this approach for malate production using fumarate as the growth-coupled substrate in *Synechocystis* mutants. A final titer of ∼1.2 mM was achieved for malate during photoautotrophic batch cultivations. Under prolonged continuous cultivation, the most efficient malate-producing strain can maintain its productivity for at least 45 generations, sharply contrasting with other producing *Synechocystis* strains engineered with classical approaches. Our study also opens a new possibility for extending the stable production concept to derivatives of growth-coupled metabolites, increasing the list of suitable target compounds.

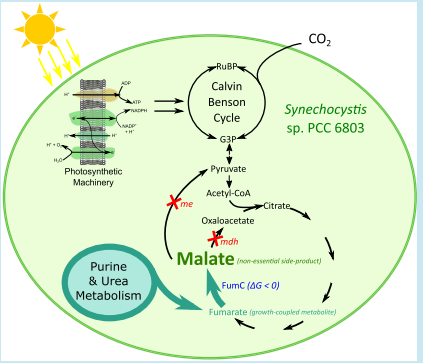

KEYWORDS: *cyanobacteria, strain stability, growth-coupled production, malate production, thermodynamically favored reactions*

INTRODUCTION

Cyanobacteria are promising microbial hosts that can be designed as cell factories to enable the development of sustainable production processes. Energized by (sun)light through their photosynthetic systems, engineered cyanobacteria can directly convert inorganic carbon dioxide into a number of chemicals such as alcohols and derived fuels (ethanol, butanol),[1,2] chemical building blocks (isoprene, lactate, polyhydroxybutyrate),[3−5] and fine chemicals.[6,7]

Classical strain improvement aims to rewire cellular metabolism to enhance the production of valuable native compounds or to endow cells with the ability to newly produce non-native ones.[8,9] However, the diversion of carbon fluxes and energy toward the production of compounds of interest implemented by the introduction and/or modification of biosynthetic pathways interferes with cellular functionalities that are subject to multilevel (e.g., proteome-, metabolic-, population-, and environmental) constraints.[10−14] The host cells could therefore experience notable pressure to opportunely reallocate resources between biomass precursors and target compound formation.[15−18] Strong evolutionary pressure favors revertant cells with impaired production, challenging the feasibility and sustainability of the industrial exploitation of cyanobacteria as cell factories.[19,20] Although negative results are seldom shown, the issue of production instability in cyanobacteria engineered to obtain valuable products such as ethylene, lactic acid, isopropanol, mannitol, and fatty acids has been reported in a handful of reports.[3,21−23]

Developing cyanobacterial-producing strains in biotechnological setups requires minimizing the negative impact of instability raised by the loss of fitness of engineered strains. Therefore, one approach is to make the growth of the engineered strain dependent on the synthesis of the compound

Received: September 3, 2021
Published: November 22, 2021

Downloaded via 87.13.3.78 on December 23, 2021 at 11:07:51 (UTC).
See https://pubs.acs.org/sharingguidelines for options on how to legitimately share published articles.

ACS Publications

© 2021 The Authors. Published by American Chemical Society

https://doi.org/10.1021/acssynbio.1c00440
ACS Synth. Biol. 2021, 10, 3518–3526

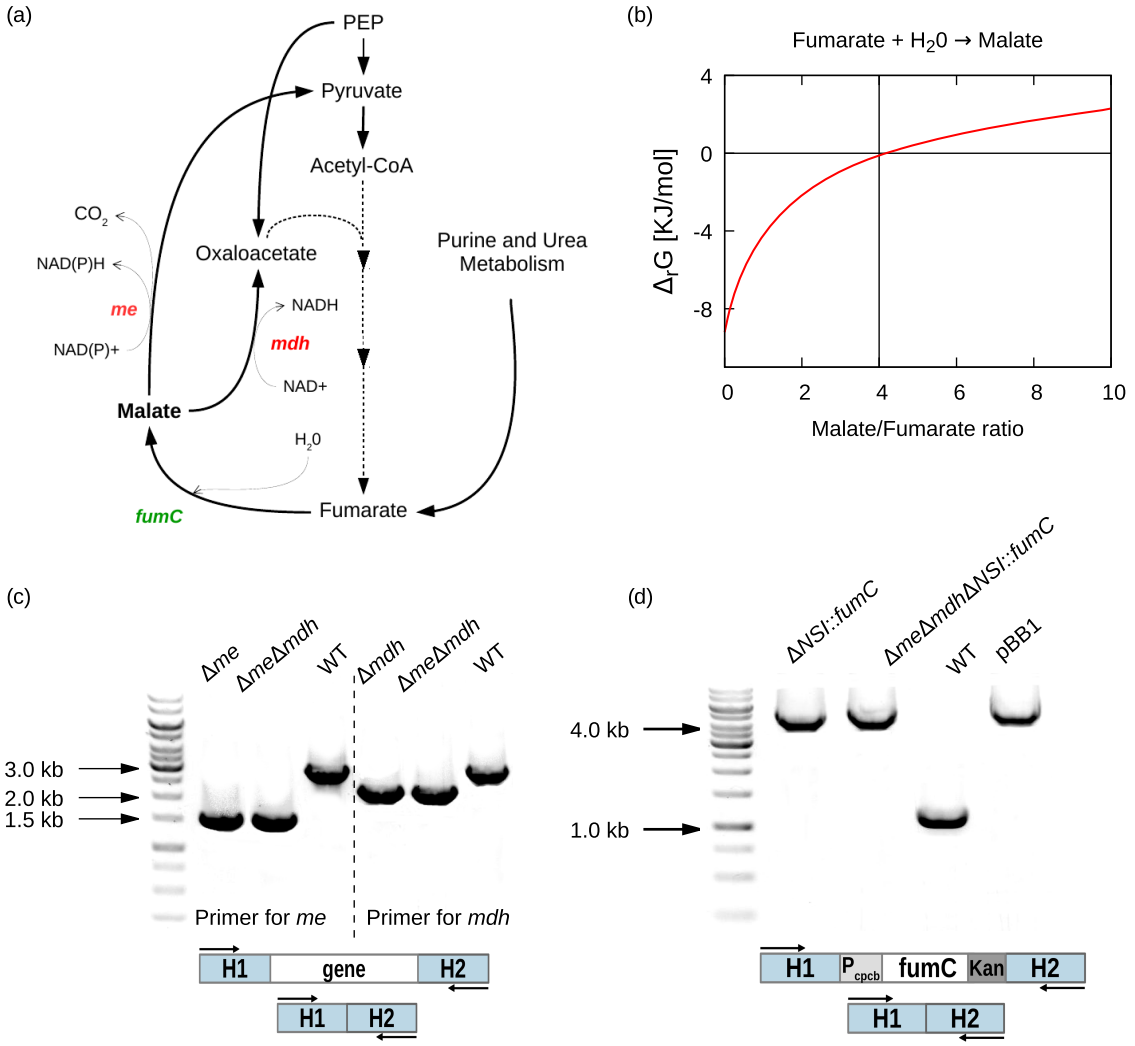

Figure 1. Malate metabolism in *Synechocystis* and mutant construction. (a) Schematic representation of malate-producing and consuming pathways, as reported by the genome-scale metabolic model (GSMM).[26] The genes deleted in this study are indicated in red, the overexpressed gene is indicated in green. (b) Thermodynamic analysis of the reaction catalyzed by the FumC. Calculations were obtained using eQuilibrator[31] for the reaction fumarate + H_2O ↔ malate. The dashed lines indicate the equilibrium point of the reaction ($\Delta G_r = 0$). (c) PCR confirmation of the strains constructed for markerless deletion of *me* and *mdh*. With the primers on each side of the upstream and downstream homologous region (H1 and H2 of ∼1 kb each), a markerless construct gave a PCR product of 1.5 and 1.8 kb for Δ*me* and Δ*mdh*, respectively. (d) PCR confirmation of the *fumC* overexpression strain. The integration of *fumC* gene in the neutral site *slr*0168 gave a PCR product of 4 kb. The genomic DNA of the WT and pBB1 were used as negative and positive controls, respectively.

that is to be produced (i.e., coupling the product forming pathway to microbial growth). In this way, the selection acting on engineered strains during their evolutionary trajectories allows producing strains to outcompete the nonproducing ones. This growth-coupled production has been implemented computationally using the FRUITS algorithm—that "Finds Reactions Usable in Tapping Side-products"—and experimentally validated in *Synechocystis* sp. PCC6803 (hereafter, *Synechocystis*) engineered to independently accumulate either acetate[24] or fumarate.[25] The biotechnologically relevant compounds obtainable through this approach are defined as the side products of anabolic pathways. Those side products can be accumulated by disrupting endogenous enzymatic reactions responsible for reintroducing them back into metabolism within a resource-efficient usage framework. In summary, the compounds resulting from this approach are growth-coupled since they are obligate side products of the formation of essential precursor metabolites. However, the number of candidates for implementing this growth-coupled strategy is limited to the metabolites that meet such criteria under the conditions for which it is determined using FRUITS. For *Synechocystis*, using model iJN678[26] constrained to simulate photoautotrophic growth, this is restricted to nine metabolites.[24]

The metabolic strategy shown in the present study broadens the aforementioned limitations inherent to the FRUITS approach. Based on a combination of metabolic modeling and genetic engineering solutions, we show how we could exploit a growth-coupled metabolite previously identified in *Synechocystis*[25] to achieve the production of a metabolite positioned immediately downstream of the growth-coupled product itself. Specifically, we report the first stable malate-producing strain of *Synechocystis* obtained by exploiting the stoichiometrically growth-coupled metabolite fumarate as a supply for the accumulation of malate, the direct subproduct of fumarate in *Synechocystis*.

https://doi.org/10.1021/acssynbio.1c00440
ACS Synth. Biol. 2021, 10, 3518−3526

Malate is a C4-dicarboxylic acid with a wide range of industrial applications since it is used as an acidulant in the feed and food industry,[27] building block for bioplastic and resin production and a component of drug delivery systems.[28] Given the manifold applications and the increasing market demand, alternative and sustainable production systems for malate are highly advisable, for instance, in a photoautotrophic host.[29]

In this study, we created the markerless deletion *Synechocystis* mutants with impaired malate consumption pathways and further improved the production by overexpressing the enzyme that converts fumarate into malate, namely, fumarase C (FumC). The rationale behind the latter is that cells would then accumulate the target product malate because (i) the reactions that consume malate have been deleted and (ii) the formation of its direct precursor, fumarate, has been previously shown to be a strict requirement for cell growth.[25] Moreover, we validated the stability of the malate production of the engineered strains over prolonged continuous cultivation. The strains obtained by implementing our new metabolic engineering strategy represent the first report of stable cyanobacterial production of malate via the conversion of the closest upstream growth-coupled compound, fumarate. It provides a starting point for the application of this novel engineering strategy to the next stages of industrial exploitation.

RESULTS AND DISCUSSION

***In Silico* Simulation for Malate Production.** In *Synechocystis* under photoautotrophic conditions, malate is exclusively produced from the precursor fumarate. The latter is mainly produced as a side product of urea and purine anabolism, and it is subsequently recycled via anaplerotic reactions. First, the FumC enzyme catalyzes the conversion of fumarate into malate (Figure 1a). Then, malate is converted either into oxaloacetate by malate dehydrogenase (Mdh) or into pyruvate by the malic enzyme (Me) through oxidative decarboxylation (Figure 1a). It has previously been demonstrated that fumarate can be produced in a growth-coupled manner, as also highlighted by the correlation existing between fumarate productivity and the growth rate of the engineered strain.[25] Considering that for *Synechocystis* fumarate is a nonessential metabolite that can be produced in a growth-coupled fashion, it is conceivable that channeling fumarate toward the accumulation of its first derivative metabolite, malate, would not cause major fitness impairments. This hypothesis is supported by Flux Variability Analysis (FVA)[30] of the genome-scale metabolic model (GSMM) of *Synechocystis* iJN678, which predicted that if enzymatic reactions are responsible for the consumption of malate are deleted, either the latter or fumarate would then be accumulated without affecting the growth capabilities. In particular, according to FVA, the single knockout of me or mdh genes would neither enhance malate accumulation nor affect *Synechocystis* growth (Tables 1 and 2), since one could take over the function of each other in simulations. On the other hand, the double deletion of the two target genes would induce the accumulation of malate up to a total amount of 0.860 mM gDW^{-1}, with a small negative effect on cell growth (Table 2). The reaction catalyzed by the FumC is reversible and, according to a biochemical thermodynamic analysis performed through eQuilibrator,[31] the conversion of fumarate into malate is allowed until the equilibrium of the reaction is reached, which corresponds to a molar ratio malate:fumarate of 4:1 under standard conditions (Figure 1b). For this reason, a residual amount of fumarate is always to be expected.

Table 1. List of Plasmids and Strains Used in This Study

plasmids and strains	description	reference
pFL-AN	BioBrick "T" vector with *Avr*II and *Nhe*I on each side	42
pWD42	Amp^rKm^r, containing the selection cassette	43
pWD71	pFL-AN derivative, Amp^r, containing *mdh* upstream and downstream homologous regions	this study
pWD72	pFL-AN derivative, Amp^rKm^r, containing the selection cassette flanked by *mdh* upstream and downstream homologous regions	this study
pWD73	pFL-AN derivative, Amp^r, containing *me* upstream and downstream homologous regions	this study
pWD74	pFL-AN derivative, Amp^rKm^r, containing the selection cassette flanked by *me* upstream and downstream homologous regions	this study
pHKH001	Amp^rKm^r, integration vector at *slr*0168 genomic locus	3
pBB1	pHKH001 derivative, Amp^rKm^r, *fumC* (from *Escherichia coli*) expressed under the cpcBA promoter	this study
Synechocystis sp. PCC6803	*Synechocystis* sp. PCC6803 wild type	D. Bhaya
WD163	*Synechocystis* sp. PCC6803 *mdh* gene knockout mutant	this study
WD169	*Synechocystis* sp. PCC6803 *me* gene knockout mutant	this study
WD170	*Synechocystis* sp. PCC6803 *mdh* and *me* gene knockout mutant	this study
WD198	*Synechocystis* sp. PCC6803 *fumC* overexpressing mutant	this study
WD199	*Synechocystis* sp. PCC6803 *mdh* and *me* gene knockout, *fumC* overexpressing mutant	this study
SAA023	*Synechocystis* sp. PCC6803 expressing L-*ldh* gene from*Lactococcus lactis*	36

To experimentally validate the feasibility of our approach by introducing the necessary genetic modifications, three markerless deletion mutants of *Synechocystis* as Δ*me*, Δ*mdh*, and Δ*me*Δ*mdh* were constructed (Figure 1c) and further characterized.

Malate Production of Δ*me*, Δ*mdh*, and Δ*me*Δ*mdh* in a Batch Photobioreactor. Growth and production capabilities of engineered and WT strains were monitored by photoautotrophic cultivation under continuous light illumination in the Multi-Cultivator. Δ*mdh* grew similarly to the WT until the end of the experiment, while Δ*me* and Δ*me*Δ*mdh* showed a measurably slower growth rate (0.052 and 0.050 h^{-1}, respectively) in the exponential phase compared to the WT (0.055 h^{-1}) (Figure 2a and Table 2). A similar negative effect on the growth rate due to the disruption of the gene encoding for the malic enzyme has been observed before.[32] Comparison of fumarate and malate extracellular production between the WT and engineered strains allowed assessing the impact of deleting *me* and *mdh* genes on the metabolism of *Synechocystis*. As expected from previous work investigating the secretion of organic metabolites by *Synechocystis* grown under photoautotrophic conditions,[33] neither fumarate nor malate was detected in significant amount in the supernatant of WT (Figure 2b,c). In contrast to the *in silico* analysis carried out, which predicted a null malate yield for the Δ*me* strain (Table 2), this mutant was able to accumulate modest amounts of malate, suggesting that the conversion of malate into oxaloacetate by Mdh is less effective than the conversion of malate into pyruvate mediated by Me. This result is in partial

https://doi.org/10.1021/acssynbio.1c00440
ACS Synth. Biol. 2021, 10, 3518−3526

Table 2. Growth Rate and Product Yields for Malate and Fumarate Relative to Biomass Either Predicted by FBA or Experimentally Observed during the Exponential Phase in Wild-Type *Synechocystis* and Derivative Strains Impaired in Malate Consumption Reactions[a]2

	growth rate (μ, h^{-1})		malate yield ($Y_{p/x}$, mM gDW^{-1})		fumarate yield ($Y_{p/x}$, mM gDW^{-1})	
strains	model prediction	measured	model prediction	measured	model prediction	measured
wild type	0.052	0.055 ± 0.001	0	0	0	0
Δ*me*	0.052	0.052 ± 0.000	0	0.067 ± 0.019	0	0.274 ± 0.014
Δ*mdh*	0.052	0.055 ± 0.000	0	0	0	0
Δ*me*Δ*mdh*	0.050	0.050 ± 0.001	0−0.860	0.607 ± 0.091	0−0.860	0.557 ± 0.002

[a]FVA was used for evaluating the robustness of the network and predicting the expected range for malate and/or fumarate production. The biomass equation was always used as the primary objective function in all FBA and FVA simulations. The experimental data are referred to the batch cultivation reported in Figure 2.

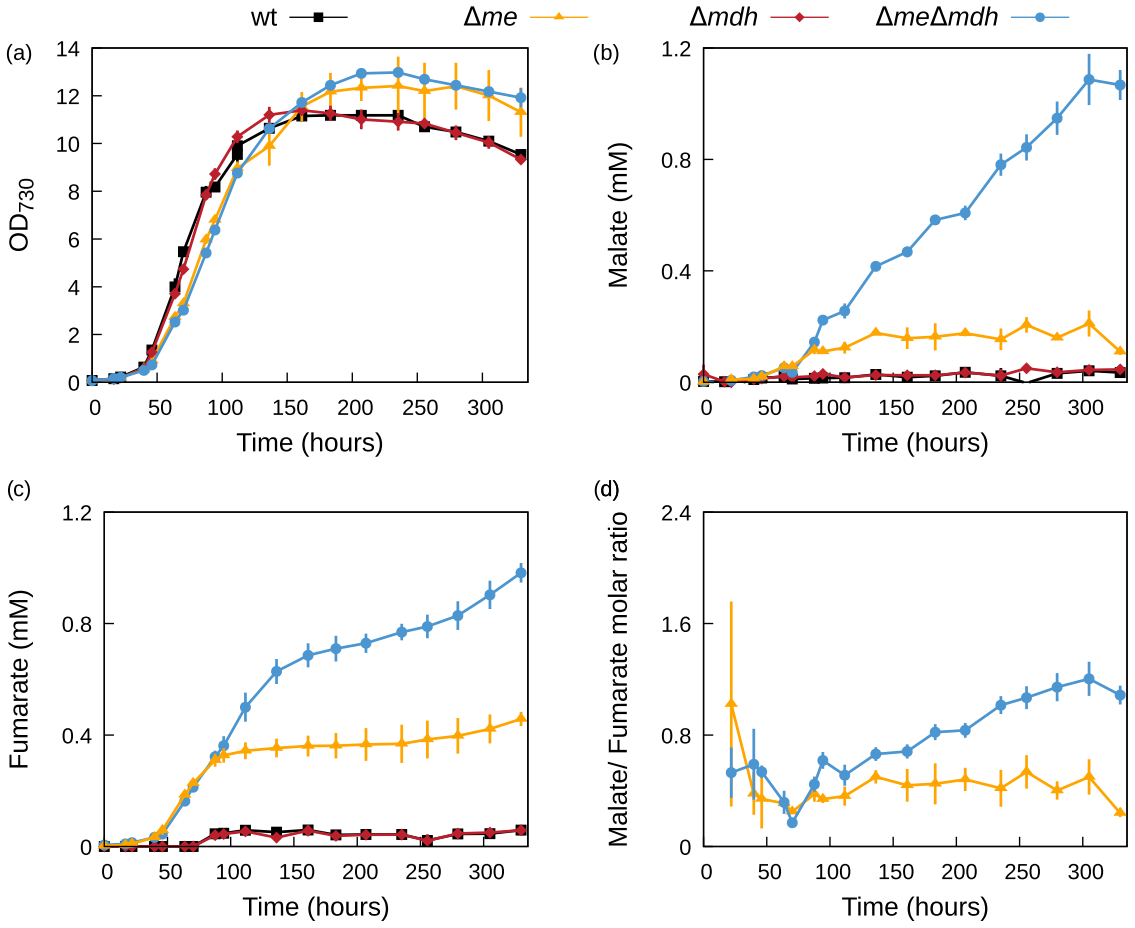

Figure 2. Characterization of *fumC* overexpressing strains of *Synechocystis* compared to the WT and to the double knockout Δ*me*Δ*mdh* cultivated under continuous light in a photobioreactor. (a) Growth curves and extracellular concentration of (b) malate and (c) fumarate of different strains. (d) Profiles of the malate/fumarate molar ratio in Δ*me* and Δ*me*Δ*mdh* strains. Values are the mean of at least two biological replicates. Error bars are standard error in panels (a)−(c) and combined standard uncertainty in panel (d). Concentration values below the detection limit of the analytical techniques used (i.e., 2 μM for malate and 20 μM for fumarate) are reported as zero in panels (b) and (c). Malate/fumarate molar ratios are not reported whenever either malate or fumarate concentration falls below the detection limit.

agreement with ^{13}C flux analysis showing that during continuous illumination, similar to that of our setup, the high levels of ATP generated inhibit the pyruvate kinase, which converts phosphoenolpyruvate (PEP) into pyruvate (Figure 1a),[34,35] inducing cells to convert malate for supplying the necessary pyruvate. In this context, indeed, the higher activity of Me compared to Mdh could be functional to provide pyruvate, thus compensating the bottleneck through the pyruvate kinase. In accordance with model predictions (Table 2), both compounds were released in the extracellular broth by Δ*me*Δ*mdh* strain, which also showed higher yields compared to Δ*me* strain (Figure 2b,c). For the Δ*me*Δ*mdh* strain, the maximum titers of malate and fumarate observed were to 1.2 and 1.0 mM, respectively, after 14 days of batch cultivation (Figures 2b,c and S1) and the maximum malate to fumarate molar ratio was about 1 (Figure 2d).

Overexpression of FumC for Improving Malate Accumulation. When considering the Δ*me*Δ*mdh* strain, which was the mutant with the highest malate production (Figures 2b and S1), the presence of a considerable amount of

https://doi.org/10.1021/acssynbio.1c00440
ACS Synth. Biol. 2021, 10, 3518−3526

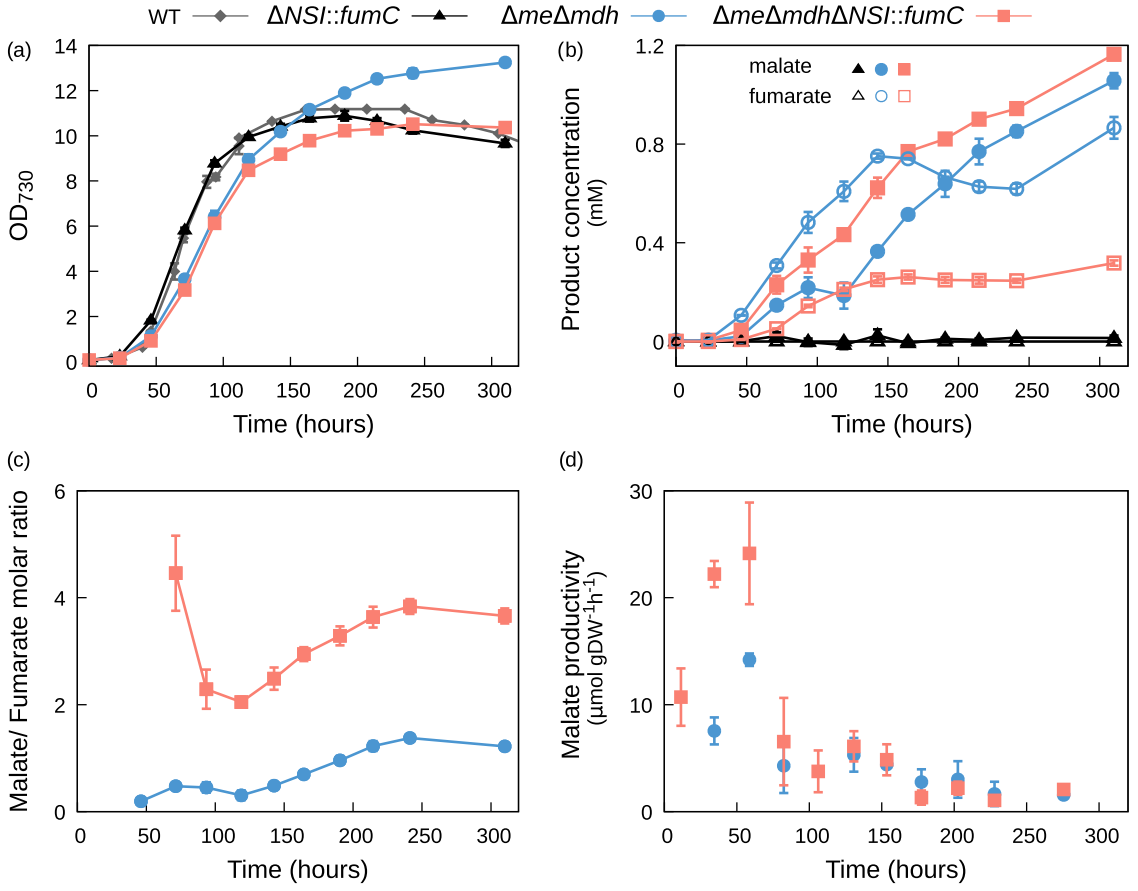

Figure 3. Characterization of *fumC* overexpressing strains of *Synechocystis* compared to the double knockout Δ*me*Δ*mdh* cultivated under continuous light in a photobioreactor. (a) Growth curves and (b) extracellular production of malate and fumarate of different strains. Variation of (c) the malate/fumarate molar ratio and (d) the malate productivity of Δ*me*Δ*mdh* and Δ*me*Δ*mdh*Δ*NSI::fumC* strains. Dry weight concentration was calculated from OD_{730} measurements using a conversion factor of 148 mg L^{-1} OD^{-1} obtained in a similar setup.[44] Values are the mean of at least two biological replicates. Error bars are standard errors in panels (a) and (b) and combined standard uncertainty in panels (c) and (d). Concentration values below the detection limit of the analytical techniques used (i.e., 2 μM for malate and 20 μM for fumarate) are reported as zero in panel (b). Malate/fumarate molar ratios are not reported whenever either malate or fumarate concentration falls below the detection limit.

fumarate in the culturing broth (Figure 2c) suggests that the intracellular conversion of fumarate into malate catalyzed by FumC might be limited. The possible enzymatic bottleneck related to the low availability of the enzyme and/or restricted access to the substrate has been explored by overexpressing *fumC*. Two strains based on the WT strain and on the background of Δ*me*Δ*mdh* mutant, i.e., Δ*NSI::fumC* and Δ*me*Δ*mdh*Δ*NSI::fumC*, have been engineered by inserting the *fumC* gene from *E. coli* in the chromosomal neutral site *slr*0168 (Figure 1d). The *E. coli fumC* gene overexpressed is only 59.4% identical to the native one of *Synechocystis*, which avoids the occurrence of undesired recombination events.

The *fumC* overexpressing strains were cultured photoautotrophically in the Multi-Cultivator under the same conditions as the deletion mutants. The growth curve of Δ*NSI::fumC* was similar to that of the WT, whereas Δ*me*Δ*mdh*Δ*NSI::fumC* showed a slower growth during the exponential phase when compared to the Δ*NSI::fumC* (Figure 3a). Conversely, Δ*me*Δ*mdh*Δ*NSI::fumC* grew similarly to the Δ*me*Δ*mdh* in the first stages of growth, reaching the steady state earlier than the double mutant (Figure 3a). Concerning malate and fumarate extracellular production, the overexpression of *fumC* alone in *Synechocystis* was not sufficient to enhance the secretion of detectable quantities of neither of the two compounds (Figure 3b). On the other hand, Δ*me*Δ*mdh*Δ*NSI::fumC* was capable of releasing in the extracellular environment higher titers of malate and lower titers of fumarate compared to the Δ*me*Δ*mdh* strain (Figure 3b; Figure S1 normalized by biomass content), determining a higher molar ratio of malate over fumarate in the extracellular broth throughout the entire cultivation (Figure 3c). When analyzing the malate productivity (calculated as the ratio between the variation of the malate production and the difference in biomass observed between two consecutive sampling points), the highest productivity was observed during the exponential phase for both the Δ*me*Δ*mdh*Δ*NSI::fumC* and Δ*me*Δ*mdh* strains (Figure 3d). In this growth phase, the malate productivity of the overexpressing triple mutant was significantly higher than that of the double deletion mutant, once more indicating an improved ability of conversion of fumarate into malate in the Δ*me*Δ*mdh*Δ*NSI::fumC* mutant.

Testing the Stability of Δ*me*Δ*mdh* and Δ*me*Δ*mdh*Δ*NSI::fumC*. The engineering approach adopted to build the Δ*me*Δ*mdh* strain is based on the removal of the two consumption pathways of malate. Cyanobacterial strains engineered adopting an analogue deletion method have been shown to be stable and productive over dozens of generations.[24,25] Consequently, also the Δ*me*Δ*mdh* strain is expected to be phenotypically stable. Most importantly, malate production should be stably maintained due to the grounds

https://doi.org/10.1021/acssynbio.1c00440
ACS Synth. Biol. 2021, 10, 3518−3526

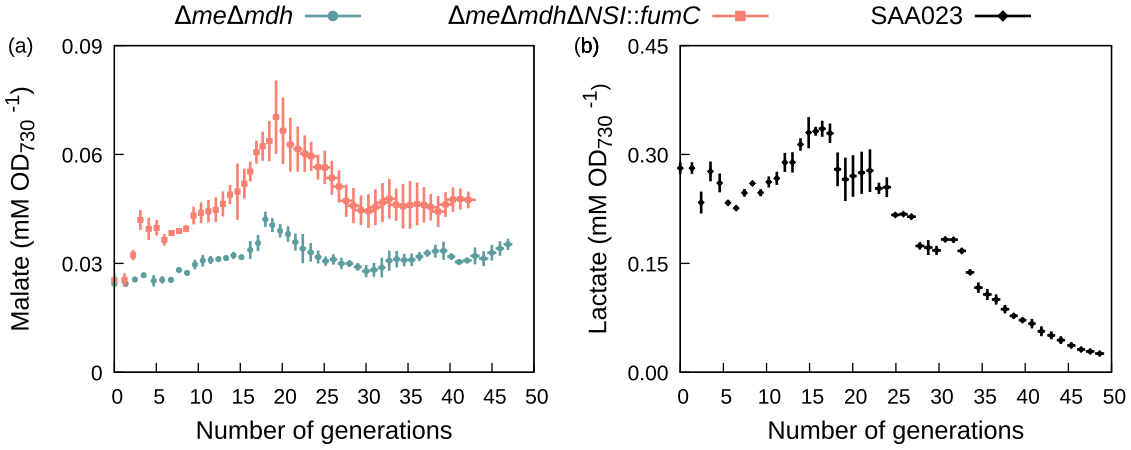

Figure 4. Malate and lactate extracellular production of different strains during the serial propagation experiment. (a) Malate production normalized by the OD_{730} of Δ*me*Δ*mdh* and Δ*me*Δ*mdh*Δ*NSI::fumC* strains. (b) Lactate production normalized by the OD_{730} of SAA023 strain. The values are the mean of three biological replicates, the *y* error bars are combined uncertainties, and the *x* error bars are standard errors.

that its precursor, fumarate, is a growth-coupled metabolite. In the Δ*me*Δ*mdh*Δ*NSI::fumC* strain, more cellular resources are involved in the synthesis of an extra amount of heterologous FumC, thus potentially introducing an additional protein burden to the cell. Therefore, assessing the phenotypic stability of this strain is of utmost pertinence.

Phenotypic stability of the most productive strains, Δ*me*Δ*mdh* and Δ*me*Δ*mdh*Δ*NSI::fumC,* was assessed through a serial propagation experiment in which cultures were kept in exponential growth (OD_{730} between ∼0.6 and 1) over a period of ∼2 months to ensure a constant selective pressure.[10] As a control strain, we used SAA023, a lactate-producing mutant of *Synechocystis*, which carries L-LDH that converts pyruvate into L-lactate.[36] SAA023 has been shown to be unstable during prolonged culturing since spontaneous revertants with mutations in the *ldh* cassette become dominants after a few generations.[15] The production instability of this strain is associated with the metabolic engineering strategy used that imposes a high trade-off between biomass growth and product formation because an essential metabolite of the central metabolism, here pyruvate, is depleted.

Throughout our laboratory evolution experiment, each culture was monitored between 42 and 50 generations, depending on the specific growth rate of the strain. Δ*me*Δ*mdh* and Δ*me*Δ*mdh*Δ*NSI::fumC* maintained a similar ability to accumulate malate in the extracellular environment until the end of their serial propagations (Figure 4a), albeit with some fluctuations along time. In contrast, a clear drop in lactate extracellular concentration was recorded for the SAA023 strain (Figure 4b). To check whether this decrease in lactate was due to the presence of mutations in the *ldh* cassette, the gene encoding for the L-LDH and the upstream promoter sequence were amplified from 15 single colonies (five from each of the three biological replicates) and subjected to Sanger sequencing. Mutations in the *ldh* cassette were found in all of the analyzed sequences (Table S2 and Figure S2). Interestingly, the mutations were found only in the coding sequence, directly hampering the correct translation of the L-LDH protein. On the other hand, no mutations were found in the *fumC* cassette tested with an analogous approach.

Taken together, these results show the promise of strategies aiming at producing compounds (here, malate) derived from growth-coupled metabolites (here, fumarate), rather than from central C-compounds necessary for growth.[24,25] The non-appearance of mutations in the *fumC* gene indicates that (i) malate and fumarate, at these concentrations, do not pose a significant challenge to be transported out of the cell; (ii) nor is the accumulation of neither of them at these levels inhibitory for the cell; and (iii) at least in the absence of nutrient limitations, the protein overexpression per se does not seem to pose a sufficiently large fitness cost for the cell. Although this finding can be somewhat unexpected a priori, it is supported by the fact that no decrease in the growth capability (Figure 3a) and no loss in malate production (Figure 4a) were recorded for the Δ*me*Δ*mdh*Δ*NSI::fumC* strain.

CONCLUSIONS

The feasibility of a metabolic engineering strategy aiming at exploiting a growth-coupled compound, fumarate, to drive the stable production of a downstream metabolite, malate, has been proved in this study. By implementing this strategy, a malate-producing strain of *Synechocystis,* Δ*me*Δ*mdh*, has been engineered. The conversion of fumarate into malate has been further improved by overexpressing heterologous FumC in the Δ*me*Δ*mdh* strain. The synthesis of an extra amount of this protein did not appear to compromise the fitness of the microorganism and did not result in a progressive loss in malate productivity due to phenotypic instability. These results indicate that the strategy proposed here in principle could be applied to other compounds deriving from a growth-coupled metabolite that is a side product of anabolism.

METHODS

***In Silico* Simulation and Tools.** The genome-scale metabolic model (GSMM) *i*JN678 was used to simulate light-limited photoautotrophic growth of *Synechocystis.* All of the details concerning the constraints imposed to perform metabolic flux analysis through flux variability analysis (FVA) and flux balance analysis (FBA)[37] are reported in ref 24. FBA and FVA were performed using PySCeS-CBMPy[38] (http://cbmpy.sourceforge.net) in combination with ILOG CPLEX Optimization Studio (IBM) under an academic license. Additional visualization of modeling simulations was carried out using a resource specifically developed for *Synechocystis*[39] available at the FAME online modeling environment.[40]

https://doi.org/10.1021/acssynbio.1c00440
ACS Synth. Biol. 2021, 10, 3518−3526

Strains and Growth Conditions. Molecular cloning was carried out in *E. coli* XL-1 blue grown at 37 °C in LB medium, either liquid in a flask with a shaking speed of 200 rpm or solidified in plates (by adding agar 1.5% w/v). To propagate a specific plasmid, the appropriate antibiotics were added to the culture medium, with a final concentration of 100 μg mL^{-1} for ampicillin and 50 μg mL^{-1} for kanamycin.

Glucose-tolerant wild-type (WT) strain of *Synechocystis* sp. PCC6803, obtained from D. Bhaya, Stanford University, Stanford, CA, was used in this study. All of the strains of *Synechocystis* (i.e., wild type and constructed mutants) have been grown in BG-11 medium[41] supplemented with 10 mM TES−NaOH (pH 8.0) as a buffer, at 30 °C in a shaking incubator (Innova 43, New Brunswick Scientific) at 120 rpm, under constant moderate white-light illumination (∼40 μmol photons m^{-2} s^{-1}, measured with a LI-250A light meter, LI-COR).

For *Synechocystis* mutants' construction, the medium was supplemented with kanamycin (final concentration of 50 μg mL^{-1}) or nickel sulfate (final concentration of 20 μM). Cell growth was monitored by measuring the optical density at 730 nm wavelength (OD_{730}) in the spectrophotometer (Biochrom WPA, Lightwave II).

Batch Cultivation. Batch cultivation experiments were carried out in a Multi-Cultivator (MC1000-OD, PSI, Czech Republic), with emitted light intensity controlled through an LED panel, equipped with "cool-white" LEDs (PSI, CZ). BG-11 supplemented with 10 mM TES−NaOH (pH 8.0) was used as a medium to grow *Synechocystis* in the reactor. The cultures grew at 30 °C bubbled with a mixture (v/v) of 99% air and 1% CO_2 supplied at a flow rate of 150 mL min^{-1}. Precultures from shake flasks (OD_{730} ∼1−1.5) were used for inoculation in the Multi-Cultivator, working with a volume of ∼60 mL (area exposed to the light = 0.0028 m^2, height of the water column = 10.32 cm) and initial OD_{730} of 0.05. After inoculation, a continuous irradiation of 30 μmol photons m^{-2} s^{-1} was applied until the cultures reached an OD_{730} of 0.6, then increased to 120 μmol photons m^{-2} s^{-1} and kept constant to the end of the experiment. Samples were collected daily and used for OD_{730} determination and product quantification in the extracellular broth.

Serial Propagation Experiments. Serial propagation experiments were performed in 100 mL Erlenmeyer flasks at 30 °C in a shaking incubator (Innova 43, New Brunswick Scientific) at 120 rpm, under constant moderate white-light illumination (∼40 μmol photons m^{-2} s^{-1}, measured with a LI-250A light meter, LI-COR). Cultures have been grown in BG-11 medium[41] supplemented with 10 mM TES−NaOH (pH 8.0) as a buffer and with kanamycin (50 μg mL^{-1}) when necessary.

Precultures derived from the original stock of each strain (OD_{730} ∼1−1.5) were used for inoculation of the experimental batches. Every strain has been tested in triplicate. Every day, each culture at OD_{730} ∼1 has been diluted to OD_{730} ∼0.6 by keeping a constant volume of 20 mL. Samples were collected at periodic intervals before the dilution procedure and used for product quantification in the extracellular broth.

The Supporting Information provides details of plasmids and generation of *Synechocystis* mutants; quantification of extracellular fumarate, malate, and lactate; malate yield on biomass; sequencing of the *ldh* and *fumC* cassettes; and sequences of the main plasmid constructs.

■ ASSOCIATED CONTENT

Supporting Information

The Supporting Information is available free of charge at https://pubs.acs.org/doi/10.1021/acssynbio.1c00440.

(i) Additional methods on the generation of plasmids and *Synechocystis* mutants; quantification of extracellular fumarate, malate, and lactate; and sequencing of the ldh and fumC cassettes; (ii) tables of the primers used in this study and the mutational analysis of the ldh expression cassette; (iii) figures of the malate yield on biomass and the identity and position of mutations found in the ldh cassete; and (iv) detailed sequence information of the cassetes used in different plasmids to obtain the *Synechocystis* mutants used in this study (PDF)

■ AUTHOR INFORMATION

Corresponding Author

Filipe Branco dos Santos − *Molecular Microbial Physiology Group, Swammerdam Institute for Life Sciences, Faculty of Science, University of Amsterdam, Amsterdam 1098 XH, The Netherlands;* orcid.org/0000-0002-4268-8080; Email: f.brancodossantos@uva.nl

Authors

Beatrice Battaglino − *Applied Science and Technology Department, BioSolar Lab, Politecnico di Torino, 10144 Torino, Italy; Centre for Sustainable Future Technologies, Istituto Italiano di Tecnologia, 10144 Torino, Italy*

Wei Du − *Molecular Microbial Physiology Group, Swammerdam Institute for Life Sciences, Faculty of Science, University of Amsterdam, Amsterdam 1098 XH, The Netherlands*

Cristina Pagliano − *Applied Science and Technology Department, BioSolar Lab, Politecnico di Torino, 10144 Torino, Italy*

Joeri A. Jongbloets − *Molecular Microbial Physiology Group, Swammerdam Institute for Life Sciences, Faculty of Science, University of Amsterdam, Amsterdam 1098 XH, The Netherlands;* orcid.org/0000-0003-3794-4120

Angela Re − *Centre for Sustainable Future Technologies, Istituto Italiano di Tecnologia, 10144 Torino, Italy*

Guido Saracco − *Applied Science and Technology Department, BioSolar Lab, Politecnico di Torino, 10144 Torino, Italy*

Complete contact information is available at: https://pubs.acs.org/10.1021/acssynbio.1c00440

Author Contributions

‖B.B. and W.D. contributed equally to this work. W.D. and F.B.d.S. first conceived this study. B.B. and W.D. carried out all experiments with the assistance of J.A.J. F.B.d.S., C.P., A.R., and G.S. provided additional supervision. B.B., W.D., and F.B.d.S. wrote the first draft. All authors read and approved the final manuscript.

Notes

The authors declare no competing financial interest.

■ ACKNOWLEDGMENTS

F.B.d.S. and W.D. were supported by the European Union's EFRO grant "Kansen voor West II." The Netherlands Organization for Scientific Research (NWO) supported

F.B.d.S. and J.A.J. through Solar-2-product grant 733 000 005. The research leading to this publication has received funding from the European Union's Horizon 2020 Research, an innovation programme under Grant Agreement No. 760994 (ENGICOIN project).

REFERENCES

(1) Gao, Z.; Zhao, H.; Li, Z.; Tan, X.; Lu, X. Photosynthetic Production of Ethanol from Carbon Dioxide in Genetically Engineered Cyanobacteria. *Energy Environ. Sci.* **2012**, *5*, 9857−9865.
(2) Liu, X.; Miao, R.; Lindberg, P.; Lindblad, P. Modular Engineering for Efficient Photosynthetic Biosynthesis of 1-Butanol from CO2 in Cyanobacteria. *Energy Environ. Sci.* **2019**, *12*, 2765−2777.
(3) Angermayr, S. A.; Paszota, M.; Hellingwerf, K. J. Engineering a Cyanobacterial Cell Factory for Production of Lactic Acid. *Appl. Environ. Microbiol.* **2012**, *78*, 7098−7106.
(4) Drosg, B.; Fritz, I.; Gattermayr, F.; Silvestrini, L. Photo-Autotrophic Production of Poly(Hydroxyalkanoates) in Cyanobacteria. *Chem. Biochem. Eng. Q.* **2015**, *29*, 145.
(5) Lindberg, P.; Park, S.; Melis, A. Engineering a Platform for Photosynthetic Isoprene Production in Cyanobacteria, Using Synechocystis as the Model Organism. *Metab. Eng.* **2010**, *12*, 70−79.
(6) Chen, G.; Qu, S.; Wang, Q.; Bian, F.; Peng, Z.; Zhang, Y.; Ge, H.; Yu, J.; Xuan, N.; Bi, Y.; et al. Transgenic Expression of Delta-6 and Delta-15 Fatty Acid Desaturases Enhances Omega-3 Polyunsaturated Fatty Acid Accumulation in Synechocystissp. PCC6803. *Biotechnol. Biofuels* **2014**, *7*, No. 32.
(7) Menin, B.; Santabarbara, S.; Lami, A.; Musazzi, S.; Villafiorita Monteleone, F.; Casazza, A. P. Non-Endogenous Ketocarotenoid Accumulation in Engineered Synechocystis Sp. PCC 6803. *Physiol. Plant* **2019**, *166*, 403−412.
(8) Davy, A. M.; Kildegaard, H. F.; Andersen, M. R. Cell Factory Engineering. *Cell Syst.* **2017**, *4*, 262−275.
(9) Lee, S. Y.; Kim, H. U. Systems Strategies for Developing Industrial Microbial Strains. *Nat. Biotechnol.* **2015**, *33*, 1061−1072.
(10) Bachmann, H.; Molenaar, D.; Branco Dos Santos, F.; Teusink, B. Experimental Evolution and the Adjustment of Metabolic Strategies in Lactic Acid Bacteria. *FEMS Microbiol. Rev.* **2017**, *41*, S201−S219.
(11) Burnap, R. L. Systems and Photosystems: Cellular Limits of Autotrophic Productivity in Cyanobacteria. *Front. Bioeng. Biotechnol.* **2015**, *3*, No. 1.
(12) Cano, M.; Holland, S. C.; Artier, J.; Burnap, R. L.; Ghirardi, M.; Morgan, J. A.; Yu, J. Glycogen Synthesis and Metabolite Overflow Contribute to Energy Balancing in Cyanobacteria. *Cell Rep.* **2018**, *23*, 667−672.
(13) Janasch, M.; Asplund-Samuelsson, J.; Steuer, R.; Hudson, E. P. Kinetic Modeling of the Calvin Cycle Identifies Flux Control and Stable Metabolomes in Synechocystis Carbon Fixation. *J. Exp. Bot.* **2019**, *70*, 973−983.
(14) Zheng, X.-y.; O'Shea, E. K. Cyanobacteria Maintain Constant Protein Concentration despite Genome Copy-Number Variation. *Cell Rep.* **2017**, *19*, 497−504.
(15) Du, W.; Angermayr, S. A.; Jongbloets, J. A.; Molenaar, D.; Bachmann, H.; Hellingwerf, K. J.; Branco dos Santos, F. Non-hierarchical Flux Regulation Exposes the Fitness Burden Associated with Lactate Production in Synechocystis Sp. PCC6803. *ACS Synth. Biol.* **2017**, *6*, 395−401.
(16) Molenaar, D.; van Berlo, R.; de Ridder, D.; Teusink, B. Shifts in Growth Strategies Reflect Tradeoffs in Cellular Economics. *Mol. Syst. Biol.* **2009**, *5*, No. 323.
(17) Nielsen, J.; Keasling, J. D. Engineering Cellular Metabolism. *Cell* **2016**, *164*, 1185−1197.
(18) Scott, M.; Gunderson, C. W.; Mateescu, E. M.; Zhang, Z.; Hwa, T. Interdependence of Cell Growth and Gene Expression: Origins and Consequences. *Science* **2010**, *330*, 1099−1102.
(19) Jones, P. R. Genetic Instability in Cyanobacteria - An Elephant in the Room? *Front. Bioeng. Biotechnol.* **2014**, *2*, No. 12.
(20) Du, W.; Burbano, P. C.; Hellingwerf, K. J.; Branco dos Santos, F. Challenges in the Application of Synthetic Biology Toward Synthesis of Commodity Products by Cyanobacteria via "Direct Conversion" BT − Synthetic Biology of Cyanobacteria. In *Advances in Experimental Medicine and Biology*; Zhang, W.; Song, X., Eds.; Springer Singapore: Singapore, 2018; pp 3−26.
(21) Kusakabe, T.; Tatsuke, T.; Tsuruno, K.; Hirokawa, Y.; Atsumi, S.; Liao, J. C.; Hanai, T. Engineering a Synthetic Pathway in Cyanobacteria for Isopropanol Production Directly from Carbon Dioxide and Light. *Metab. Eng.* **2013**, *20*, 101−108.
(22) Jacobsen, J. H.; Frigaard, N. U. Engineering of Photosynthetic Mannitol Biosynthesis from CO2 in a Cyanobacterium. *Metab. Eng.* **2014**, *21*, 60−70.
(23) Yunus, I. S.; Jones, P. R. Photosynthesis-Dependent Biosynthesis of Medium Chain-Length Fatty Acids and Alcohols. *Metab. Eng.* **2018**, *49*, 59−68.
(24) Du, W.; Jongbloets, J. A.; van Boxtel, C.; Pineda Hernández, H.; Lips, D.; Oliver, B. G.; Hellingwerf, K. J.; Branco dos Santos, F. Alignment of Microbial Fitness with Engineered Product Formation: Obligatory Coupling between Acetate Production and Photo-autotrophic Growth. *Biotechnol. Biofuels* **2018**, *11*, No. 38.
(25) Du, W.; Jongbloets, J. A.; Guillaume, M.; van de Putte, B.; Battaglino, B.; Hellingwerf, K. J.; Branco dos Santos, F. Exploiting Day- and Night-Time Metabolism of Synechocystis Sp. PCC 6803 for Fitness-Coupled Fumarate Production around the Clock. *ACS Synth. Biol.* **2019**, *8*, 2263−2269.
(26) Nogales, J.; Gudmundsson, S.; Knight, E. M.; Palsson, B. O.; Thiele, I. Detailing the Optimality of Photosynthesis in Cyanobacteria through Systems Biology Analysis. *Proc. Natl. Acad. Sci. U.S.A.* **2012**, *109*, 2678−2683.
(27) Thakker, C.; Martínez, I.; Li, W.; San, K. Y.; Bennett, G. N. Metabolic Engineering of Carbon and Redox Flow in the Production of Small Organic Acids. *J. Ind. Microbiol. Biotechnol.* **2015**, *42*, 403−422.
(28) Zou, X.; Cheng, C.; Feng, J.; Song, X.; Lin, M.; Yang, S. T. Biosynthesis of Polymalic Acid in Fermentation: Advances and Prospects for Industrial Application. *Crit. Rev. Biotechnol.* **2019**, *39*, 408−421.
(29) Hu, G.; Zhou, J.; Chen, X.; Qian, Y.; Gao, C.; Guo, L.; Xu, P.; Chen, W.; Chen, J.; Li, Y.; et al. Engineering Synergetic CO2-Fixing Pathways for Malate Production. *Metab. Eng.* **2018**, *47*, 496−504.
(30) Mahadevan, R.; Schilling, C. H. The Effects of Alternate Optimal Solutions in Constraint-Based Genome-Scale Metabolic Models. *Metab. Eng.* **2003**, *5*, 264−276.
(31) Flamholz, A.; Noor, E.; Bar-Even, A.; Milo, R. EQuilibrator - The Biochemical Thermodynamics Calculator. *Nucleic Acids Res.* **2012**, *40*, D770−D775.
(32) Bricker, T. M.; Zhang, S. L.; Laborde, S. M.; Mayer, P. R.; Frankel, L. K.; Moroney, J. V. The Malic Enzyme Is Required for Optimal Photo Autotrophic Growth of Synechocystis Sp Strain PCC 6803 under Continuous Light but Not under a Diurnal Light Regimen. *J. Bacteriol.* **2004**, *186*, 8144−8148.
(33) Young, J. D.; Shastri, A. A.; Stephanopoulos, G.; Morgan, J. A. Mapping Photoautotrophic Metabolism with Isotopically Nonstationary 13C Flux Analysis. *Metab. Eng.* **2011**, *13*, 656−665.
(34) Wan, N.; DeLorenzo, D. M.; He, L.; You, L.; Immethun, C. M.; Wang, G.; Baidoo, E. E. K.; Hollinshead, W.; Keasling, J. D.; Moon, T. S.; et al. Cyanobacterial Carbon Metabolism: Fluxome Plasticity and Oxygen Dependence. *Biotechnol. Bioeng.* **2017**, *114*, 1593−1602.
(35) Jazmin, L. J.; Xu, Y.; Cheah, Y. E.; Adebiyi, A. O.; Johnson, C. H.; Young, J. D. Isotopically Nonstationary 13C Flux Analysis of Cyanobacterial Isobutyraldehyde Production. *Metab. Eng.* **2017**, *42*, 9−18.
(36) Angermayr, S. A.; Hellingwerf, K. J. On the Use of Metabolic Control Analysis in the Optimization of Cyanobacterial Biosolar Cell Factories. *J. Phys. Chem. B* **2013**, *117*, 11169−11175.

https://doi.org/10.1021/acssynbio.1c00440
ACS Synth. Biol. 2021, 10, 3518−3526

(37) Orth, J. D.; Thiele, I.; Palsson, B. O. What Is Flux Balance Analysis? *Nat. Biotechnol.* **2010**, *28*, 245−248.
(38) Olivier, B. G.; Rohwer, J. M.; Hofmeyr, J. H. S. Modelling Cellular Systems with PySCeS. *Bioinformatics* **2005**, *21*, 560−561.
(39) Maarleveld, T. R.; Boele, J.; Bruggeman, F. J.; Teusink, B. A Data Integration and Visualization Resource for the Metabolic Network of Synechocystis Sp. PCC 6803. *Plant Physiol.* **2014**, *164*, 1111−1121.
(40) Boele, J.; Olivier, B. G.; Teusink, B. FAME, the Flux Analysis and Modeling Environment. *BMC Syst. Biol.* **2012**, *6*, No. 8.
(41) van Alphen, P.; Abedini Najafabadi, H.; Branco dos Santos, F.; Hellingwerf, K. J. Increasing the Photoautotrophic Growth Rate of Synechocystis Sp. PCC 6803 by Identifying the Limitations of Its Cultivation. *Biotechnol. J.* **2018**, *13*, No. 1700764.
(42) Zhu, T.; Xie, X.; Li, Z.; Tan, X.; Lu, X. Enhancing Photosynthetic Production of Ethylene in Genetically Engineered Synechocystis Sp. PCC 6803. *Green Chem.* **2015**, *17*, 421−434.
(43) Carpine, R.; Du, W.; Olivieri, G.; Pollio, A.; Hellingwerf, K. J.; Marzocchella, A.; Branco dos Santos, F. Genetic Engineering of Synechocystis Sp. PCC6803 for Poly-β-Hydroxybutyrate Overproduction. *Algal Res.* **2017**, *25*, 117−127.
(44) Du, W.; Jongbloets, J. A.; Pineda Hernandez, H.; Bruggeman, F. J.; Hellingwerf, K. J.; Branco dos Santos, F. Photonfluxostat: A Method for Light-Limited Batch Cultivation of Cyanobacteria at Different, yet Constant, Growth Rates. *Algal Res.* **2016**, *20*, 118−125.

https://doi.org/10.1021/acssynbio.1c00440
ACS Synth. Biol. 2021, 10, 3518−3526